SPE-214062-MS

An Experimental Study on the Effect of Gas on the Performance of a Multi-parallel Pipe Oil-Water Separator (MPPS)

Hamidreza Asaadian and Milan Stanko, Norges teknisk-naturvitenskapelige universitet - NTNU

 DOI 10.2118/214062-MS

This paper was prepared for presentation at the Gas & Oil Technology Showcase and Conference held in Dubai, UAE, 13 - 15 March, 2023.

Abstract

This work presents a comprehensive experimental study on the effect of gas on the performance of oil-water bulk separation in a multi-parallel pipe separator (MPPS). Several flowrates of gas, up to 10% volume fraction were tested and values of separation efficiency and water cut ratio were estimated from measurements. Also, the three-phase flow pattern upstream the separator inlet is reported.

Exxsol D60 spiked with 700 ppm of crude oil, 3.4 wt% NaCl saltwater, and air were used in steady-state and transient tests on a transparent 6.1 m long, 15.24 cm diameter, separator prototype. Preliminary values of separation efficiency and water cut ratio were measured over a variety of total flow rates (300 to 700 L/min), water cuts (WC, 30%, 50%, 70%, and 90%), and water extraction rates (ER, 50% to 90% the rate of inlet water)

It is observed that the gas phase accumulates at higher sections of the separator (i.e. at the inlet section after the splitting and at the exit section where water rich fluid is tapped from the bottom of the pipe). It seems the reduction in separation performance is due to turbulence caused by the gas and reduced cross section for the oil-water mixture to flow. The higher the gas flow rate, the lower the separation efficiency and water cut ratio. The presence of gas impacts more flow conditions with low water cuts including 30 and 50%. The presence of gas has less negative impact on separator performance when the liquid flow rate is high. Results show even small amounts of gas entering the separator have a significant detrimental effect on oil-water separation.

Pipe oil-water separators have several advantages over heavy gravity vessels, including cost, compactness, ease of deployment and enable energy saving by separating close to the source. However, this study shows that the presence of gas can impact dramatically their performance. Thus, the performance of upstream gas separation must be studied closely.

Introduction

In offshore oil and gas fields, the separation process has traditionally taken place topside, alongside other processing equipment. However, there has been a push in the last decade to relocate processing equipment to the ocean floor. As topside offshore footprints become increasingly limited and subsea technology advances, a new market for subsea processing systems is arising (Prescott, Mantha et al. 2016). As the amount of

produced water in mature oil fields grows, it becomes increasingly important to separate the ever-increasing volumes of water from the oil at subsea and inject it into a suitable formation (Shi, Xu et al. 2012, Asaadian, Soltani Soulgani et al. 2018).

The separation of well fluid at the ocean floor has several advantages, the first of which is flow assurance. Subsea separation improves flow control and mitigates flow assurance issues associated with multiphase flow, such as hydrate formation, slugging, and pressure loss (da Silva, Monteiro et al. 2013). Furthermore, the seabed provides more physical room for large, heavy processing equipment, freeing up space on the topside for additional tiebacks. Operators can now exploit longer tiebacks to reservoirs that were previously unattainable or uneconomical to produce due to improved flow conditions and increased topside capacity (Shi, Xu et al. 2012, Asaadian and Soltani Soulgani 2019).

The implementation of subsea processing, like any new technology, is filled with challenges. Many of these issues are imposed by the subsea environment. High seafloor pressures limit vessel size and necessitate a very robust engineering design; thicker vessel walls significantly increase the weight and cost of subsea equipment. Another issue to consider when dealing with the ocean environment is corrosion. Finally, the technical challenge of designing subsea equipment to operate autonomously with minimal maintenance and intervention exists (Fantoft 2005, Gruehagen and Lim 2009).

For topside separation, large, horizontal, gravity-based separation vessels have been the industry standard. These vessels, however, can become very heavy in the subsea environment. There has recently been a push to develop linear, pipe-based subsea separators. A separator with a pipe classification requires a much smaller wall thickness than a comparable vessel-based separator at the same operating pressure, as required by many offshore codes and standards. Separators based on pipe classification can be made lighter and less expensive; they can be fabricated from standard pipe sizes, resulting in lower costs due to the high availability of base materials and ease of fabrication. (Prescott, Mantha et al. 2016, Skjefstad and Stanko 2018).

Based on these advantages, Skjefstad et al. proposed the Multi Parallel Pipe Separator (MPPS), a separator design for bulk oil-water separation that uses multiple parallel branches (Skjefstad and Stanko 2017). When compared to existing subsea bulk-water separator installations, the concept employs numerous pipes in tandem, resulting in shorter settling periods and a more compact, modularized, and flexible separator design (Stanko and Golan 2015).

This work studies the effect of the presence of small amounts of gas on separation process in MPPS. The separator is designed to be installed downstream of a gas separation unit and it only handles oil and water. However, such gas separation units are often not 100% efficient and small amounts of gas usually enter the oil-water separator. As a result, this inquiry is required for further advancement of the MPPS concept's Technological Readiness Level. Therefore, small amounts of gas (up to 10% gas volume fraction) were introduced to the inlet flow to evaluate the effect of gas on separation efficiency and water cut ratio. Drainage potential curves for all gas flow conditions are compared with separation with no gas. Finally, fundamental driven mechanism during the separation process with presence of gas is described and investigated.

Methods and Materials

Experiments were performed using the same facilities used by Skjefstad which are placed at department of geoscience and petroleum, NTNU in Trondheim (Skjefstad and Stanko 2018). The comprehensive details are presented in Skjefstad (2019) article (Skjefstad and Stanko 2019), however some specifics and recent extensions are described here for clarity. Figure 1 illustrates the experimental facilities' process and instrumentation diagrams. This system contains a large storage tank (6 m3) for the base separation, two small and two large centrifugal pumps, pipes, valves, and pressure and flow meters. In this process, oil and water streams are drained from the storage tank tap points, pumped, measured, and then merged into one meeting point to make liquid-liquid mixture stream. Afterward, the gas phase introduced to the main

flowline. After passing through VT.1, a control valve that is always fully open, the mixture stream then passes onto a prototype separator that separates water from oil and gas.

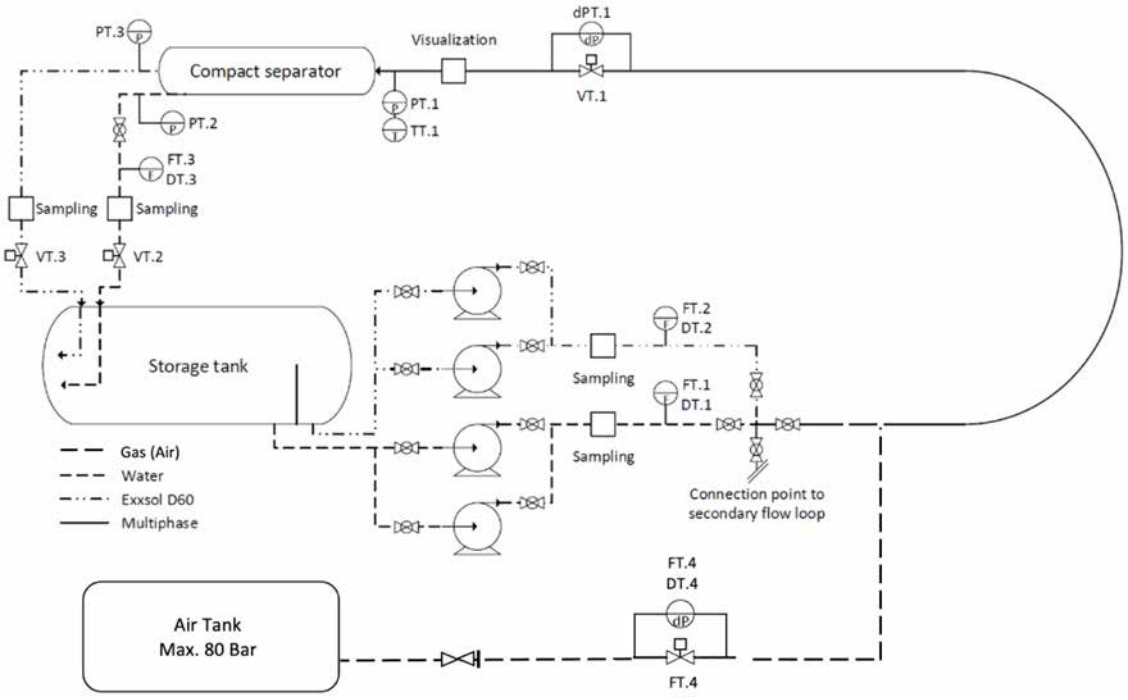

Figure 1—Experimental setup PI&D map

Adjusting the frequency of the pumps controls the inflow oil and water rates, as well as the water cut. The rate of gas phase is measured and adjusted by Coriolis flowmeter FT.4 and control valve VT.4, respectively, to reach maximum 10% of volume fraction. Control valves VT.3 and VT.2 gradually open and close to control the rates of the separate streams (oil-rich and water-rich). The pressure is measured at the separator's inlet and outlet, as well as at the inlet control valve (VT.1). Two Coriolis flowmeters (FT.1, FT.2) installed before the merge point measure and monitor the rates and water fractions of the inlet streams. A Coriolis flowmeter located at the aquatic stream's outlet is used to monitor and record the flow rate and water fraction.

A detailed schematic of MPPS prototype is illustrated in Figure 2. As it is illustrated, mixture stream enters the separator by tangential inlet which helps with pre-separation (1). Afterward, the T-junction header inlet splits the mixture stream into each branch of the separator. Then a descending pipe section conduct the flow to the horizontal pipe section (2). The horizontal mid-section has length of 3.5 m and diameter of 150.6 mm and is mainly responsible for phase separation driven by gravitational force and density difference (3,4). While the flow is entering to the ascending pipe section the water-rich stream is tapped from the tapping point close to the bottom of the ascending section (5). The oil-rich scream contained with gas, flows, and exits from the other outlet at the end of ascending section (6).

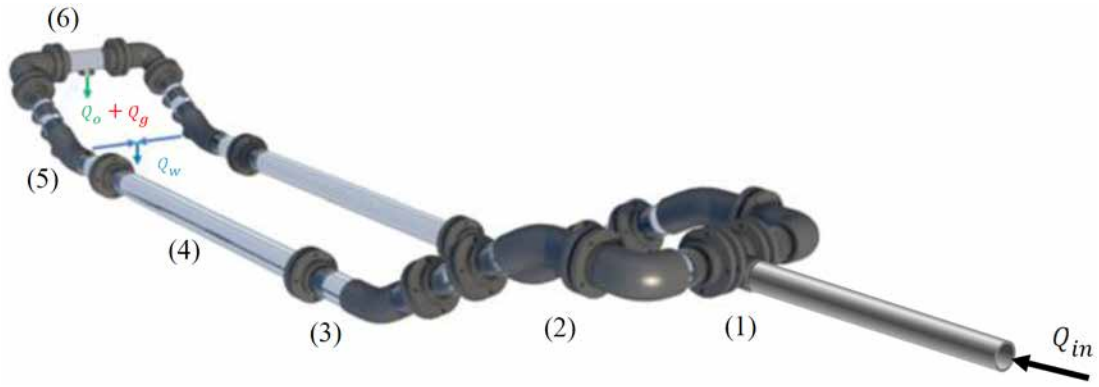

Figure 2—MPPS prototype

The experimental fluids are Exxsol D60 and distilled water with 3.4 wt% NaCl. Exxsol D60 contains trace amounts of the colorant Oil Red O (C26H24N4O), for better visualization and crude oil. In the experiments, mixture of saltwater and Exxsol D60 blended with real crude oil is used. To mimic the separation characteristics of real crude oil mixtures, small quantities of real crude is added to the Exxsol D60, a process called "crude oil spiking". Additionally, air is employed as gas phase in experimental campaigns. Fluids and crude properties at 15°C are given in Table 1. Model fluid was prepared by 400 ppm of crude oil spiking with Exxsol D60.

Table 1—Fluid Properties

Fluid	Density [kg/m³]	Viscosity [cP]
Distilled Water w/ *wt%* 3.4 NaCl	1023.7	0.99
Exxsol D60 w/ 0.015 *g/L* Oil Red O	796.2	1.41
Crude Oil	939.1	224.01

This subsection introduces the terms that are used for evaluating the separation process at different flow conditions.

Drainage potential curve:

This concept was initially introduced by Stanko and Golan (2015) and then investigated in MPPS by Asaadian et al. (2022) (Stanko and Golan 2015). As shown in Figure 3, a mixture of oil and water enters the separator at a flow rate of total liquid $\dot{Q}$total with water fraction (also called water cut) WC_{inlet}. The tapping point points downward, removes water and some oil, while an oil-rich stream exits rightward. The tapped stream has a water rate $\dot{Q}_{water\ tapped}$, a total tapped liquid flow rate $\dot{Q}_{tapped}{}^{tapped}$, and a water fraction WC_{tapped}. Pipes can be horizontal or inclined upwards or downwards.

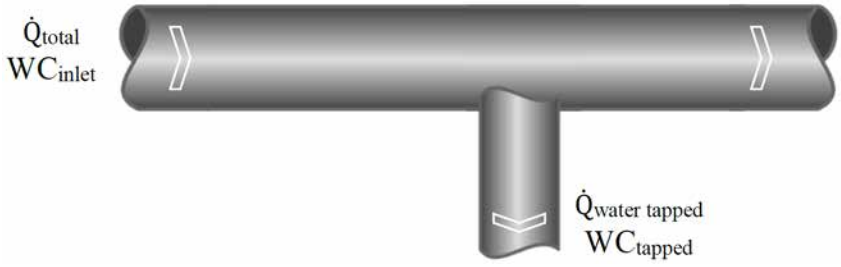

Figure 3—Tapping of stream

As shown in Equation 1, the efficiency of the tapping point (Water tapped (WT)) can be expressed as the proportion of the total water flow that was tapped compared to the inlet water flow.

$$WT[\%] = \frac{\dot{Q}_{watertapped}}{\dot{Q}_{water}} \times 100 \tag{1}$$

The drainage potential represents the relationship between the water cut of a tapped stream WC_{tapped} and the tapped water flow (WT). There are several factors that affect this relationship, including the rate and properties of oil and water, the pipe size, angle, and material, and the position and configuration of the tapping point. Figure 4 illustrates an example of drainage potential curve (Asaadian, Harstad et al. 2022). As indicated in the figure, approximately 40% of the inlet water rate can be drained before oil is noticeably drained.

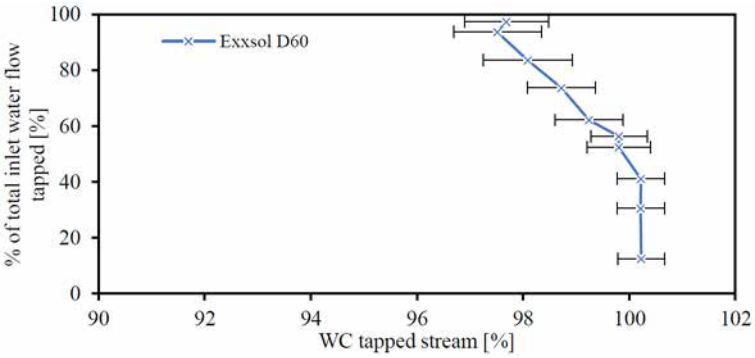

Figure 4—Drainage potential curve

Separation efficiency:

Equation 3 allows to estimate the water cut of the inlet stream, where the volumetric flows through each feed line are $\dot{Q}_1$ and $\dot{Q}_2$ and the calculated water cuts of water and Exxsol D60 feed lines are WC_1 and WC_2. Each feed line's water cut was calculated using Equation 2. According to the experiments, the water cut of the water line is practically equal to one and the water cut of the oil line is practically equal to zero. However, as a result of poor separation in the storage tank, there is a possibility that the pure water and pure oil lines could be contaminated with oil and water, respectively.

$$WC_i = \frac{\rho_i - \rho_o}{\rho_w - \rho_o} \tag{2}$$

$$WC_{in} = \frac{WC_1\dot{Q}_1 + WC_2\dot{Q}_2}{\dot{Q}_1 + \dot{Q}_2} \tag{3}$$

At fixed extraction rates (ER), separation efficiencies are estimated and reported. A water outlet ER is calculated by dividing the tapped total liquid rate by a water inlet flow rate (Equation 4).

$$ER = \frac{\dot{Q}_3}{\dot{Q}_1} \tag{4}$$

Calculating separation efficiency requires dividing the rate of water extraction by the potential amount of water that can be removed at a given ER, as it is shown in Equation 5.

$$\varepsilon = \frac{WC_3\dot{Q}_3}{ER(WC_{in}(\dot{Q}_1 + \dot{Q}_2))} \tag{5}$$

Water cut ratio:
Exxsol D60 will disperse in the inflow water over time, causing phase contamination. This might result in a separation efficiency greater than 1. The ratio of water cut at the water extraction line versus the WC at the water input line was further calculated, in addition to separation efficiency (Equation 6). High separation efficiency is indicated by a ratio equal to one.

$$WC_{ratio} = \frac{WC_3}{WC_1} \times 100 \tag{6}$$

An experimental campaign with four water cuts, three total liquid flow rates, and six different gas flow rates was conducted, totaling 72 points. The gas flowrate varies from 0 to 0.6, 1.6, 3.3, 6.6 and 10% of total liquid flowrate. The gas flowrates are introduced to the system at ambient temperature 25°C and 1.5 bar pressure. The Gas Volume Fraction (GVF) is reported as a proportion of the total volumetric flow at actual pipe conditions. An overview of the test matrix can be found in Table 2.

Table 2—Experimental campaign test matrix

Total liquid flowrate [L/min]	Water cut [%]	Gas flowrate [L/min]
300	30/50/70/90	0/2/5/10/20/30
500	30/50/70/90	0/3.4/8.4/16.7/33.4/50
700	30/50/70/90	0/4.7/11.7/23.4/46.7/70

Results and Discussion

All mechanisms that effect separator performance are discussed here. Based on observations and measurements, four different phenomena influence the efficiency of separation process along the MPPS. Gas accumulates at downward inclined section and at the beginning of the horizontal section, decreasing the effective horizontal pipe cross section, causing high turbulency at tapping point and cyclic gas release at oil outlet.

Gas pocket at downward inclined section and at the beginning of the horizontal section
As it is shown in Figure 5a when the flow conditions at MPPS reach a steady state and stable conditions, a gas pocket forms at the highest elevated section of MPPS (T-section) (Section 2 in Figure 2). The gas pocket then pushes the liquid level down into the downward inclined section toward the horizontal section. Higher gas flowrates result in bigger gas pockets closer to horizontal section. In some cases (liquid flowrate equal to 700 L/min and high GVF), the gas pocket breaks through into the horizontal section as presented in Figure 5b (section 3 in Figure 2).

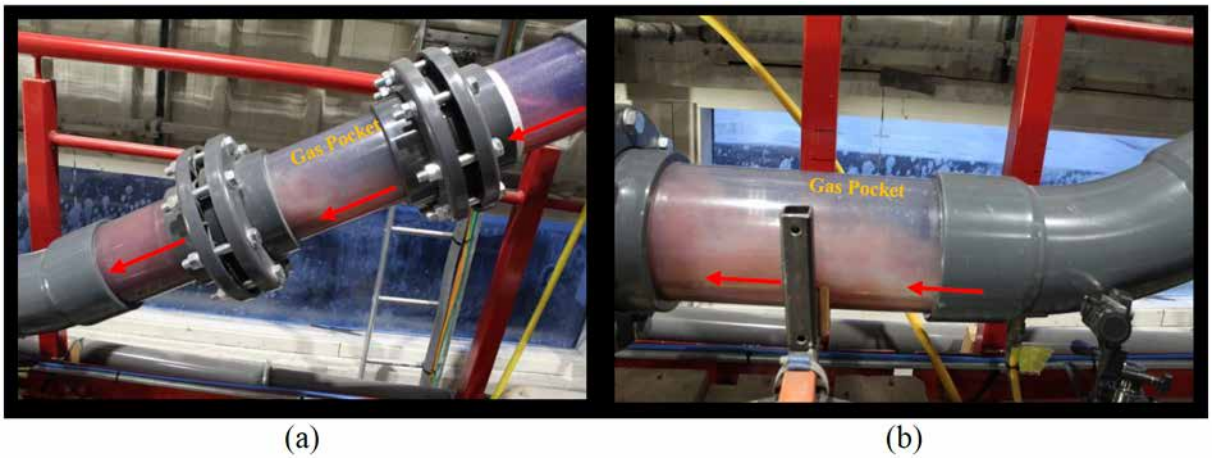

Figure 5—Gas pocked at a) downward inclined section and b) at the beginning of the horizontal section

Decreasing the effective horizontal pipe cross section

Whether there is a gas pocket breakthrough or not into the horizontal section, gas typically flows through the horizontal section, reaches the top of the ascending section and is released from the oil outlet. Therefore, that volume of the pipe which is occupied by gas phase will affect the separation process along the horizontal section, as the oil-water mixture has a smaller pipe cross section to flow through and flow at higher velocities, which is detrimental for separation (section 4 in Figure 2). This problem has higher impact at higher GVF (Figure 6).

Figure 6—Decreasing the effective horizontal pipe cross section

High turbulency at tapping point

When the liquid and gas flowrates are high, three phase mixture is dispersed enough that the residence time is not sufficient for complete gas separation close to the tapping point and there are some gas bubbles nearby to the bottom of the pipe (section 5 in Figure 2). The drag force brings the gas droplets with tapped water stream. This phenomenon is called gas breakthrough and is observed mostly at conditions with high GVF, and lowest WC_{inlet} 30%.

Cyclic gas release at oil outlet

The gas phase movement from the end of the horizontal section to the end of ascending section is cyclic process. As soon as the gas layer pressure is enough to overcome the hydrostatic pressure of the ascending section, gas starts flowing through the upward inclined pipe and accumulates above the oil outlet. The same process is happening for gas release from oil outlet (section 6 in Figure 2). Figure 7 shows the pressure change at oil outlet for flowing conditions, total liquid flowrate 300 L/min, WC_{inlet} 50% and three different

gas flow rates 10, 20 and 30 L/min. This figure shows the cyclic behavior of this phenomena. Also, it indicates high gas flow rates result in higher pressures at oil outlet.

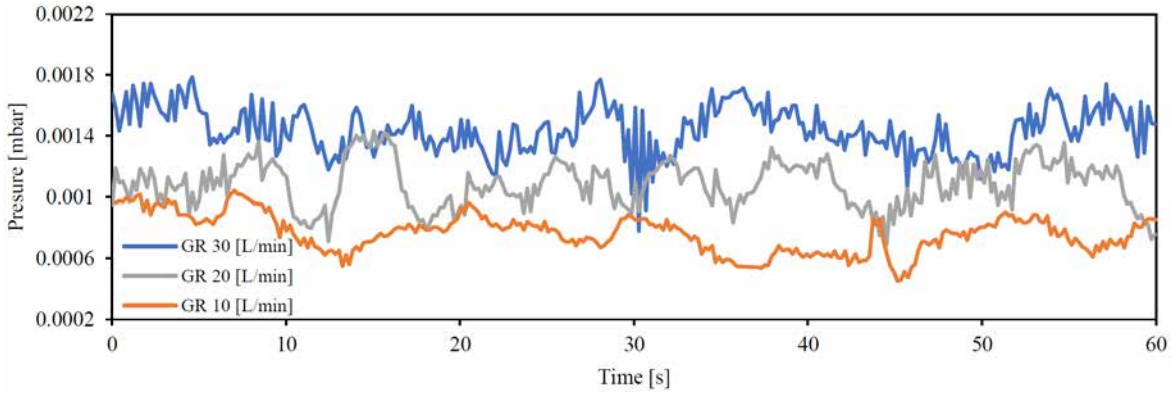

Figure 7—Pressure changes of oil outlet for different gas rates 10, 20 and 30 L/min

Figure 8 shows the same variables and conditions shown in Figure 7 but plotted separately. As it is shown the frequency of the described phenomena is decreased when the gas rate increases. The cycle period time is changed from 11 to 6.6 and 13.2 with increasing the gas flow rate from 10 to 20 and 30 L/min.

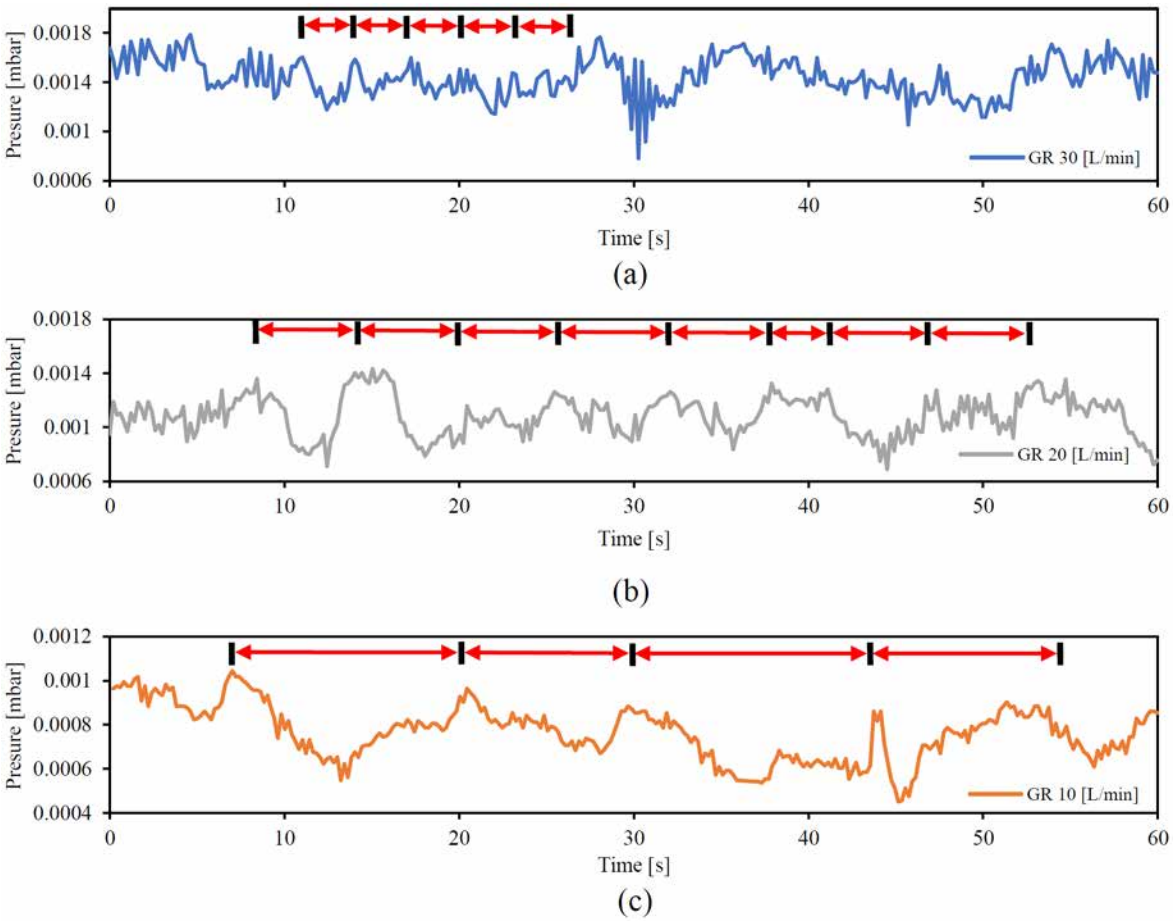

Figure 8—Pressure changes of oil outlet for different gas rates a)10, b)20 and c)30 L/min

Separation Efficiency and Water Cut Ratio

The measured separation efficiencies for the experimental campaign are presented in this section. Initially, the separation efficiency is plotted against gas flow rate for the same total liquid flowrate (but different water cuts). This illustrates the effect of adding oil on the separation performance with presence of gas. Then, the separation efficiencies are displayed for fixed water cut but varying the total liquid flowrate. This is to explore how the separation efficiency is affected by changes in the total liquid flow rate. Extraction rate for all the following curves is set to 90%. In Figure 9a, the total liquid flowrate is equal to 300 L/min. The presence of gas does not have any significant effect on separation efficiency for WC_{inlet}s 90 and 70% and the separation efficiency remains above than 98%. It means the separator is able to handle small amounts of gas up to 10% GVF without any interruption in separation process. Meanwhile, for lower WC_{inlet}s 50 and 30% the separation efficiency experiences a sudden drop after when introducing the lowest amount of gas (= 2 L/min). Increasing the gas flow rate from 10 to 30 does not make major change on separation efficiency.

Figure 9b displays the separation efficiencies for total liquid flowrate 500 L/min. With the decrease in water cut, the reduction in separation efficiency due to the presence of gas becomes more pronounced. For WC_{inlet} equal to 90% the absolute drop in efficiency between the no gas and 50 L/min gas flow is below than 2%. On the other hand, that difference is around 50% for WC_{inlet} 30%. Similar to condition with total liquid flowrate 300 L/min, the sudden drop in efficiency with the lowest gas flowrate 2 L/min is noticeable for WC_{inlet}s equal to 50 and 30% but the efficiency decreasing continuous in higher gas flowrates. Values of separation efficiency versus gas rate for a total liquid flowrate 700 L/min are shown in Figure 9c. The separation efficiency is gradually reduced by increasing gas flowrate for WC_{inlet}s 90, 70 and 50%. For WC_{inlet} 30%, the reduction of efficiency has a similar same behavior, but there is a sudden drop when small amounts of gas are introduced. In general, most of the significant reductions in separation efficiency occur for the two lowest water cuts 50 and 30%.

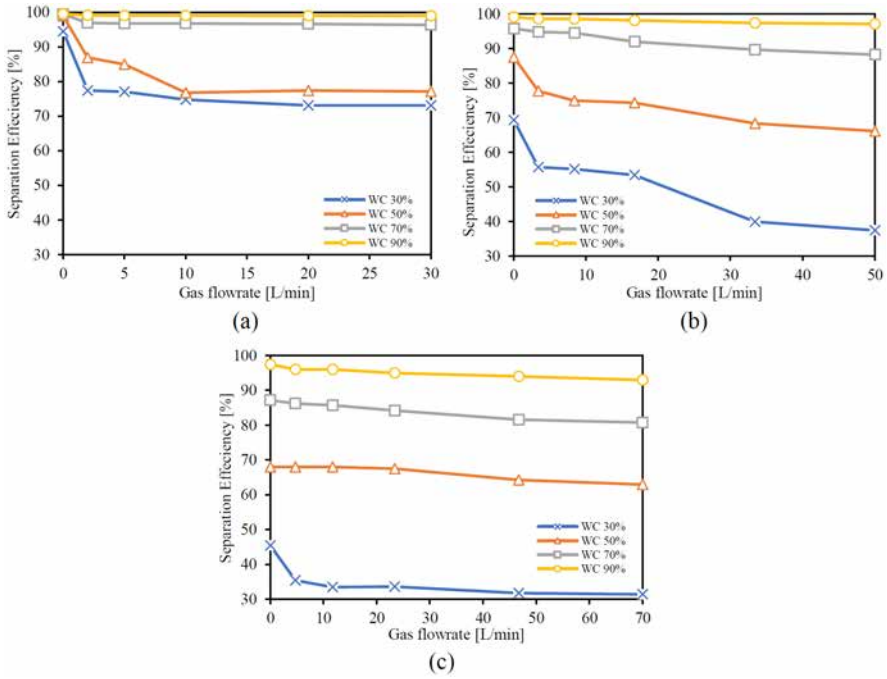

Figure 9—Effect of gas flowrate on separation efficiency for different total liquid flowrate a)300, b)500 and c)700 L/min

Figure 10 displays the separation efficiencies versus gas flow rate for constant values of WC_{inlet}. Each figure shows the separation efficiencies for total liquid flowrates of 300, 500 and 700 L/min. According to Figures 10a and 10b, the reduction in separation efficiency is most severe at total liquid flowrates 300

and 500 L/min. Nevertheless, when the WC_{inlet} increased to 70 and 90% (Figure 10c and 10d) the biggest reduction in separation efficiency due to the presence of gas is biggest at the highest total liquid flowrate 700 L/min. Most of the significant loss in separation efficiency occurs for the two lowest WC_{inlet}s, 50 and 30%. The same trend is observed in all cases: There is a detrimental effect on separation efficiency when gas flowrates are high.

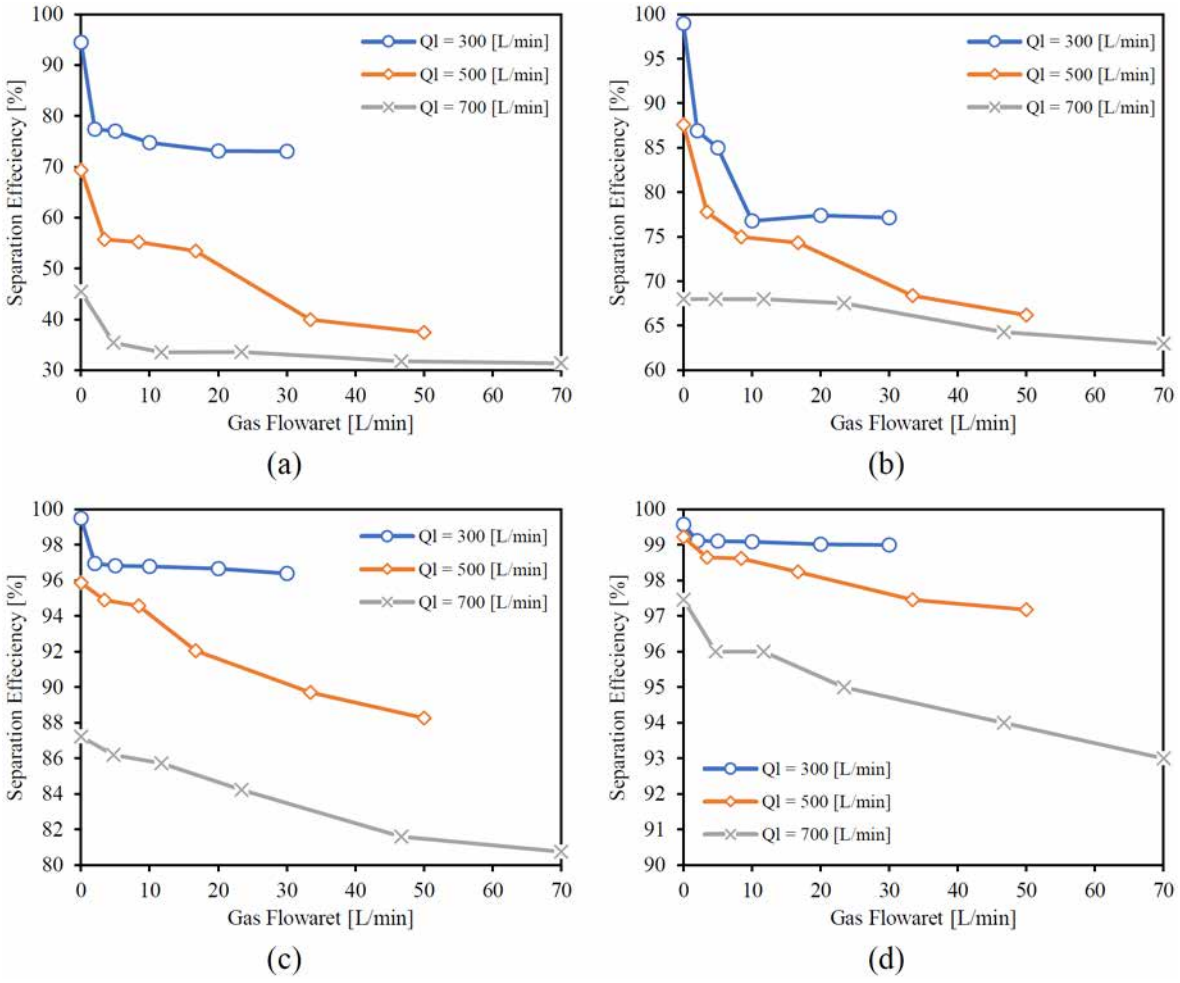

Figure 10—Effect of gas flowrate on separation efficiency for different total liquid flowrate and water cuts a)30, b)50, c)700 and d)90%

The main purpose of adding crude spiking and introducing the gas phase to the system was to measure the performance of the pipe separator under more realistic separation characteristics. The crude spiking is supposed to mimic separation characteristics of the crude-saltwater liquid system at 60°C (Asaadian, Harstad et al. 2022). The gas phase is added to evaluate the effect of residual gas on liquid-liquid separation. Figure 11 illustrated the separation efficiency and water cut ratio evolution during changes in fluid system.

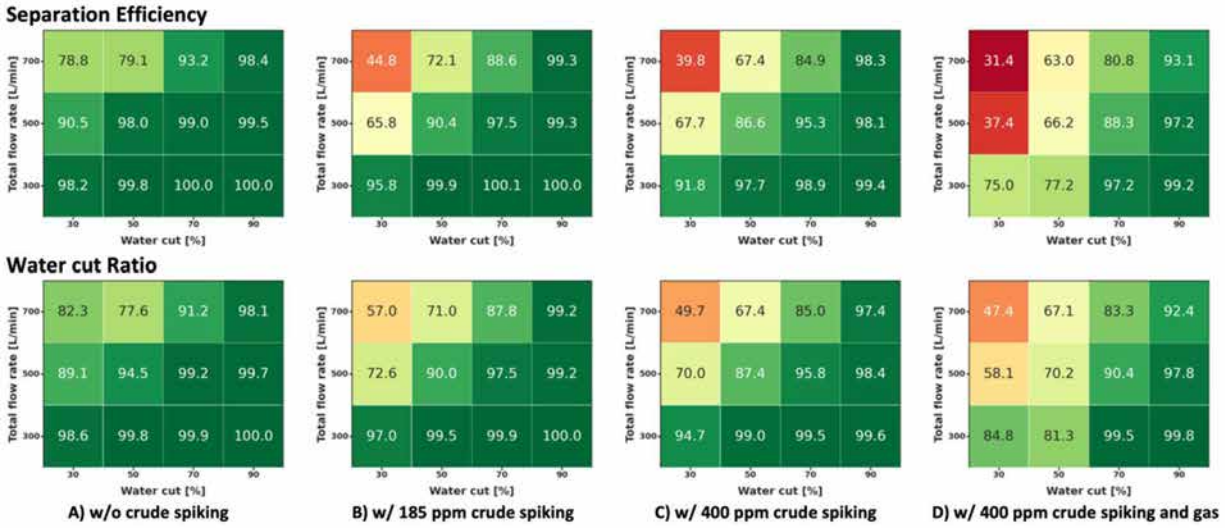

Figure 11—Separation efficiency and water cut ratio for different fluid system a)w/o crud spiking, b) w/ 185 ppm crude spiking, c)w/400 ppm crude spiking, d)w/ 400 ppm crude spiking and10% GVF gas

The separation efficiency and water cut ratio reduces with adding crude spiking especially for conditions with low WC_{inlet} and high total liquid flowrate (oil continuous flow regime). With compression of figures 11a with 11b and 11c, the highest reduction belongs to WC_{inlet} 30% and total liquid rate 700 L/min. The same tendency is noticeable when the gas phase enters to the system with 10% GVF (Figure 11d).

Drainage Potential Curve

This section presents the drainage potential curves calculated from experimental values. For no gas and for gas flows up to 10% GVF, the drainage potential curves will be shown under the same inlet conditions, i.e., WC_{inlet} and total inlet liquid rate. An illustration of the effect of adding the gas phase on the tapping point's separation performance is shown here.

After that, the drainage potential curves are displayed for inlets with a fixed WC_{inlet} and inlets with variable liquid and gas flow rates. The purpose of this is to illustrate how changes in the total liquid and gas inlet rate affect the drainage potential curves. This work computes drainage potential curves for two parallel tapping points. The drainage potential curve for both tapping points is considered similar with assuming they behave identically.

Comparison between drainage potential curves for no gas and various gas flowrates at the same inlet conditions

Figure 12 shows the drainage potential curves for a total flow rate of 300 L/min and WC_{inlet} values of 30% (Figure 12a), 50% (Figure 12b), 70 % (Figure 12c), and 90% (Figure 12d) for the various flowrates of gas phase from 0 to 10% GVF. A photo of the flow pattern with no gas flow condition downstream of the tapping point can also be found in figure 12d.

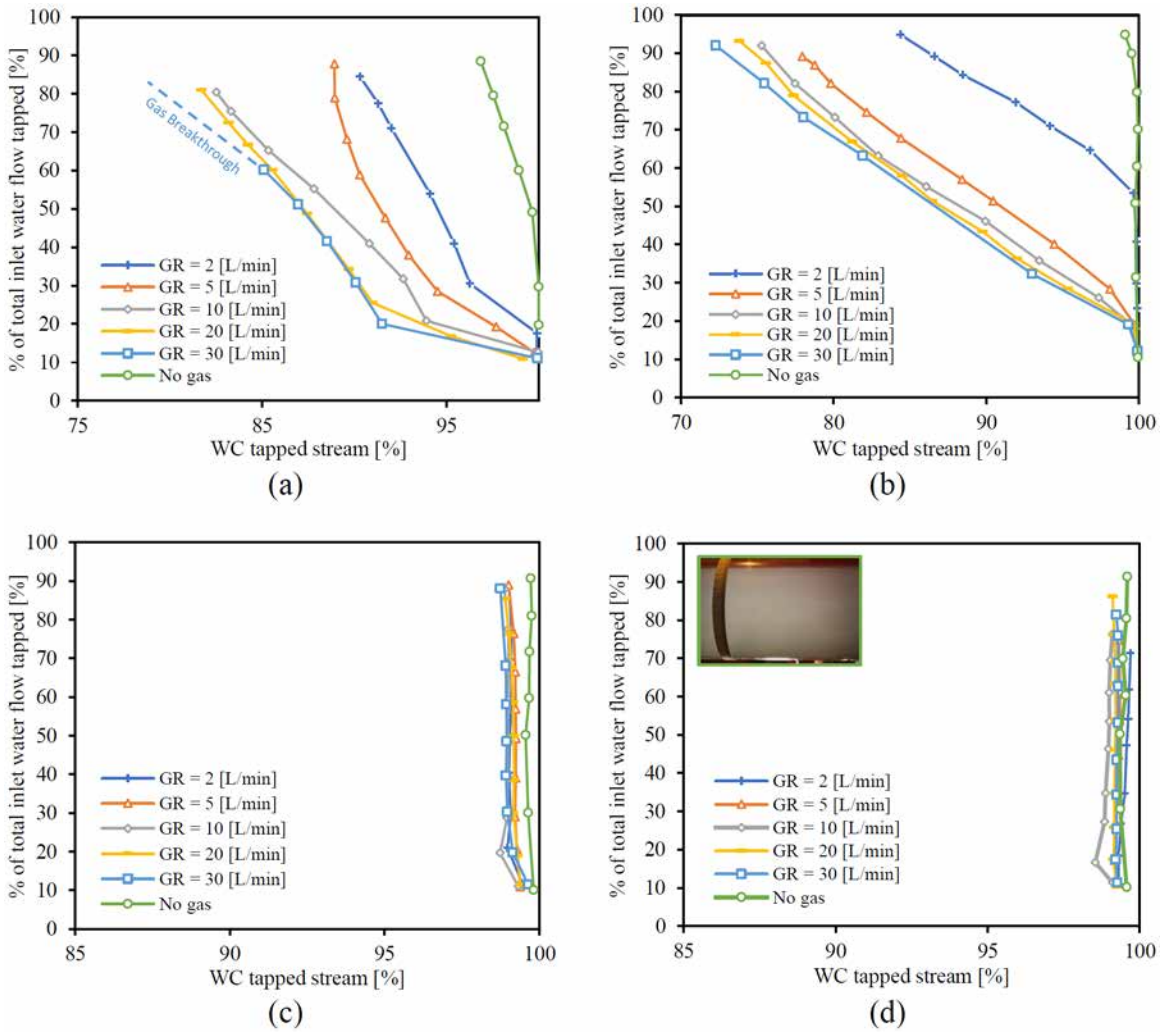

Figure 12—Drainage potential for no gas and various gas flowrates with total liquid flow rate of 300 L/min, at WC_{inlet} (a) 30%, (b) 50%, (c) 70%, and (d) 90%

For the cases with water cut 70 and 90%, it is possible to tap large amounts of water without tapping large amounts of oil and there is no significant difference between drainage potential curve with and without the presence of gas. The water cut of tapped stream will remained above than 98% (curves are generally vertical). For WC_{inlet} 50% the drainage potential curve for no gas flow condition remains vertical but adding gas decreases the threshold WT at which oil starts to be tapped from 50 for 2 L/min gas rate to 10% for higher gas rates. For a WC_{inlet} of 30%, the drainage potential curves show worse separation performance at low WT compared to WC_{inlet} 50%. Gas breakthrough (gas flowing through the water outlet) is observed for 30 L/min gas flowrate and when tapping more than 60% inlet water rate.

In all conditions of no gas flow illustrated in Figure 12, there are no visible dispersion layers, and the flow pattern is O & W. Perhaps this explains why significant amounts of water can be drained without extracting significant amounts of oil. When gas is introduced, it causes the formation of a dispersion layer which hinders from tapping pure water.

Drainage potential curves for different GVFs are shown in Figure 13 for a total flow rate of 500 L/min and WC_{inlet} values of 30%, 50%, 70%, and 90% respectively. Also included in figure 13 are photos of the flow pattern upstream of the tapping point at no gas flow condition.

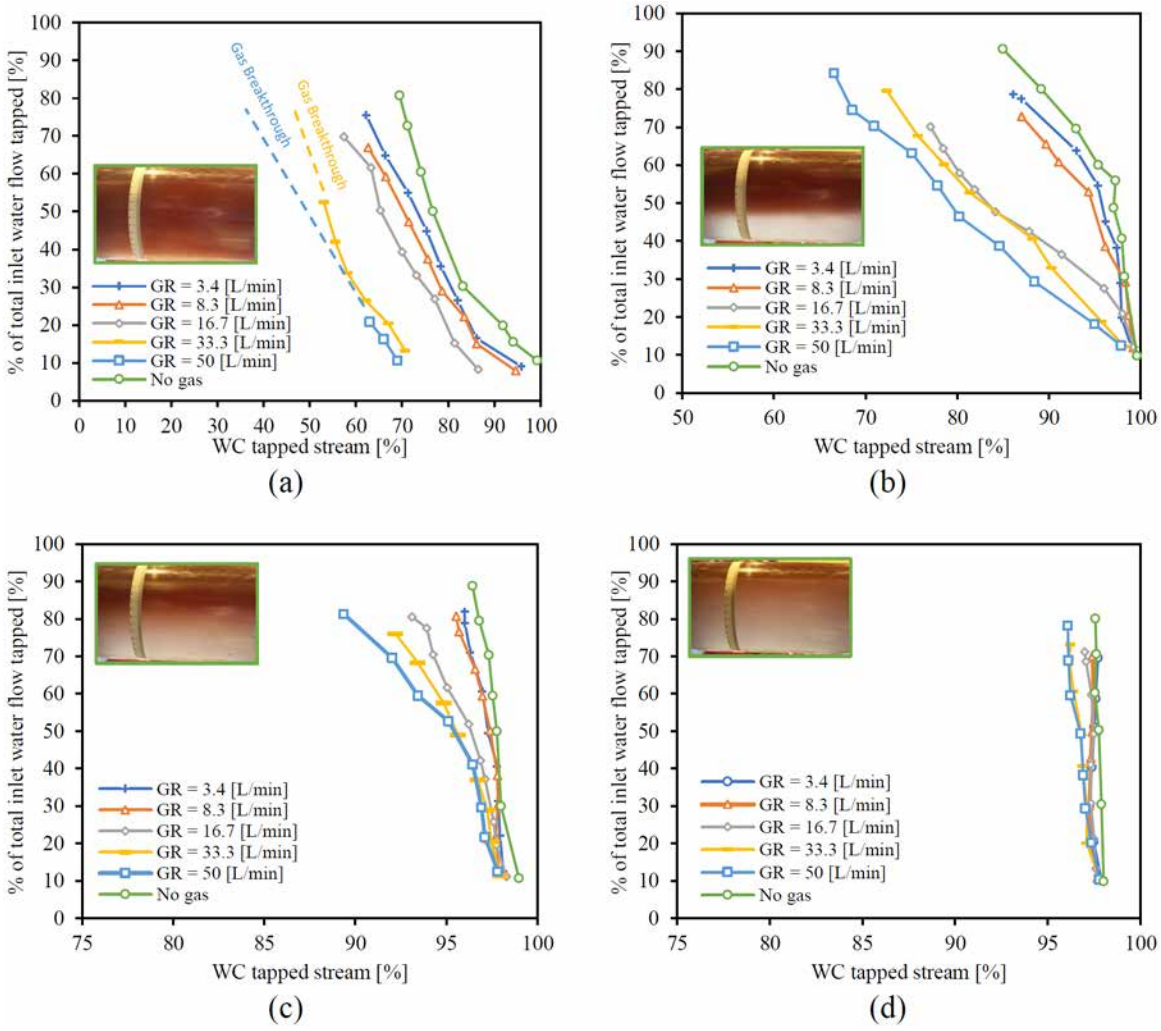

Figure 13—Drainage potential for no gas and various gas flowrates with total liquid flow rate of 500 L/min, at WC_{inlet} (a) 30%, (b) 50%, (c) 70%, and (d) 90%

WC_{inlet} values of 70 and 90% result in a low amount of oil tapped up to WT values of 90% when there is no gas in the pipe. According to the photos, the flow pattern approaching the tapping point consists of O&W with a thick water layer, so it seems that most of the water is transported in this layer and tapped from it (Figure 13c and 13b). The presence of gas does not affect significantly this behavior for WC_{inlet} 90%, but it has a significant detrimental effect for WC_{inlet} 70%.

Drainage potential curves with WC_{inlet} values of 30 and 50% with no gas, show a decline in the water cut of tapped streams as WT increases (Figure 13a and 13b). For a WC_{inlet} of 50%, the decrease in WC of the tapped stream versus WT is sharper than WC_{inlet} of 70%. Based on the photo, the flow pattern upstream the tapping point is O and Dw/o and W. With the water cut of the tapped stream declining at values of WT greater than 50%, It seems the remaining water is dispersed in the oil. Presence of gas seems to increase the thickness of this layer, resulting in lower WC_{tapped}.

As oil contamination in water layer increases, WC_{tapped} on the x-axis decreases. When WC_{inlet} is 30%, the flow regime is O & Dw/o & Do/w. When the gas rate increases, it results in more oil contamination in taped water stream (lower WC_{tapped} for the same WT). However, all the drainage potential curves have the same trend. The gas breakthrough is observed at lower WT (20%) for 10% GVF and started at 6.6% GVF around 52% WT.

Drainage potential curves for no gas and different gas rates are illustrated in Figure 14 with WC_{inlet} values of 30% (Figure 14a), 50% (Figure 14b), and 70% (Figure 14c) for total liquid rate 700 L/min. A few photos of the flow pattern upstream of the tapping point are included in Figure 14 when there is no gas in separator.

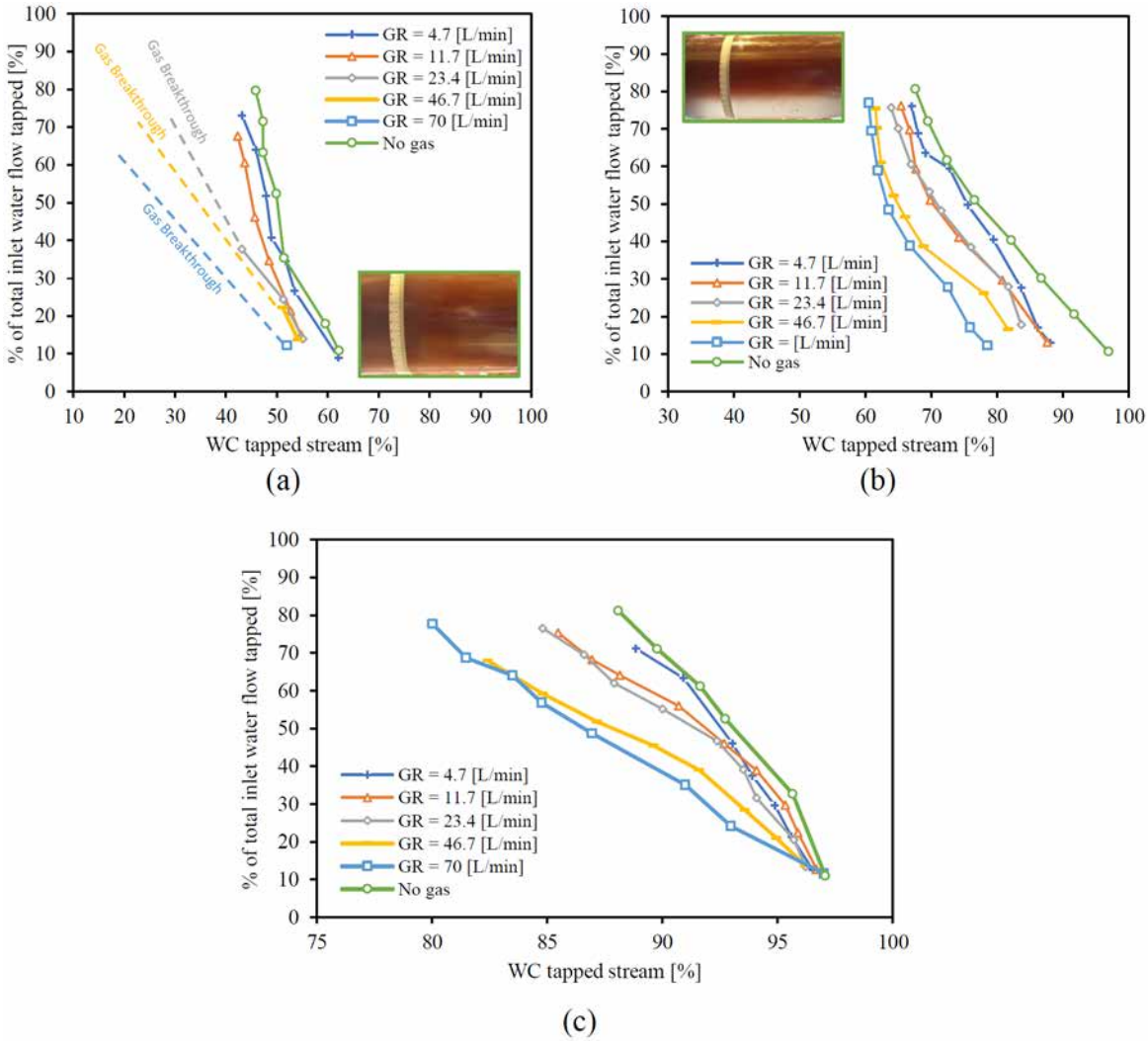

Figure 14—Drainage potential for no gas and various gas flowrates with total liquid flow rate of 700 L/min, at WC_{inlet} (a) 30%, (b) 50%, and (c) 70%

When the value of WC_{inlet} is 30%, the liquid-liquid flow regime is O & Dw/o. Tapped water is contaminated with oil even for the lowest value of WT. High rate of fluids results in earlier gas breakthrough at 6.6 and 10% GVFs and observable in lower GVF of 3.3% from around WT of 37%.

At 50% WC_{inlet}, the flow pattern appears to be O & Dw/o & W. The water cut of the tapped stream declines steadily with WT, suggesting that only a small amount of water is transported at the bottom of the pipe. Adding gas to the system causes more oil to be dispersed at the bottom of the pipe, which results in lower values of WC_{tapped}.

Behavior of drainage potential curves for inlets with a fixed WC_{inlet} with different liquid and gas flow rates

Figures 15a, 15b, 15c, and 15d show drainage potential curves for values of WC_{inlet} of 30%, 50%, 70%, and 90%. For each figure, drainage potential curves are presented for flow rates of 300, 500, and 700 L/min, and for no gas and 10% GVF conditions. All figures indicate that higher gas and liquid flowrates negatively

affect the drainage potential curve. Additionally, when the WC_{inlet} is 30%, there is a high chance of gas breakthrough for high total liquid rates.

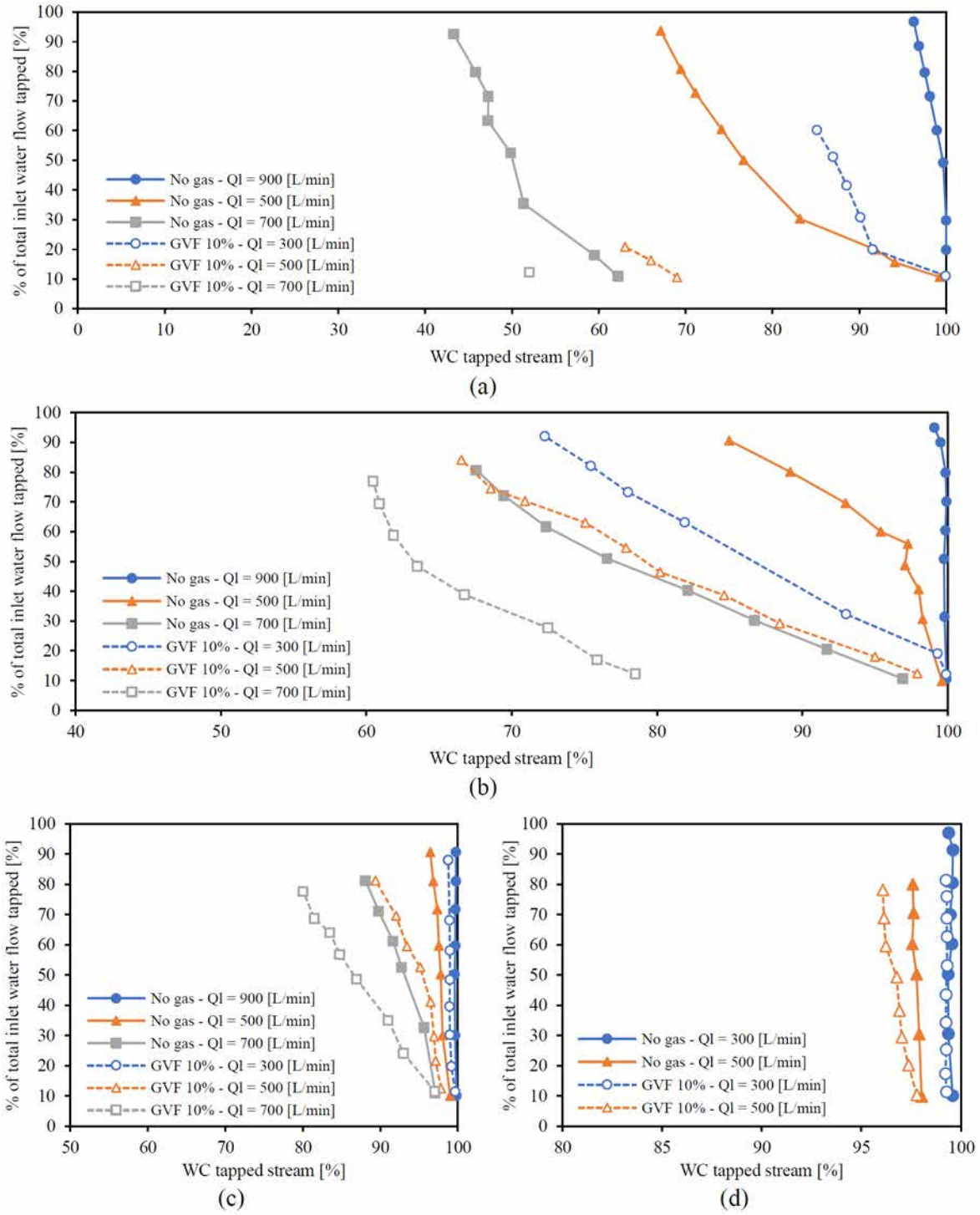

Figure 15—Drainage potential for no gas and 10% GVF at WC_{inlet} (a) 30%, (b) 50%, and (c) 70% and d)90%

Conclusion

The presence of gas causes the occurrence of several phenomena inside the MPPS (formation of a gas pocket in the downcomer, flow of gas in the horizontal and upward section, turbulence in the vicinity of the tapping point and accumulation at the oil outlet) that is detrimental for its separation performance.

The maximum reduction in separation efficiency was recorded at a total liquid flow rate of 700 L/min. Likewise, significant separation efficiency losses occur for the two lowest values of WC_{inlet}, i.e. 50 and 30%. The effect was less noticeable for high water cut values and lower liquid rates.

According to experimental drainage potential curves, high inlet water cuts and low flow rates are associated with better separation efficiency (e.g., increasing the amount of clean water that can be extracted). Meanwhile increasing the total liquid flowrate and water cut inlet make the performance more sensitive to the presence of gas.

Acknowledgement

This work was done as a part of SUBPRO, a research-based innovation center for subsea production and processing. The Department of Geoscience and Petroleum, NTNU, the Research Council of Norway, and key industry partners all contributed financially to SUBPRO, which the authors gladly acknowledge. The authors also acknowledge senior engineer, Noralf Vedvik, for his valuable support.

References

- Asaadian, H., S. Harstad and M. Stanko (2022). "Drainage Potential Curves of Single Tapping Point for Bulk Oil-Water Separation in Pipe." *Energies* **15**(19): 6911.
- Asaadian, H. and B. Soltani Soulgani (2019). "Experimental Investigation of Gas/Liquid Cylindrical Cyclone Separator." *Journal of Petroleum Research* **29**(98-2): 112–124.
- Asaadian, H., B. Soltani Soulgani, S. Rezaei Gomari and B. Soltani Soulgani (2018). Experimental investigation over effect of geometrical changes on gas/liquid cylindrical cyclone GLCC separator. Abu Dhabi International Petroleum Exhibition & Conference, OnePetro.
- da Silva, F. S., A. S. Monteiro, D. A. de Oliveira, C. A. Capela Moraes and P. M. Marins (2013). Subsea versus topside processing-conventional and new technologies. *OTC Brasil*, OnePetro.
- Fantoft, R. (2005). Subsea gas compression-challenges and solutions. Offshore Technology Conference, OnePetro.
- Gruehagen, H. and D. Lim (2009). Subsea separation and boosting—An overview of ongoing projects. Asia Pacific Oil and Gas Conference & Exhibition, OnePetro.
- Prescott, N., A. Mantha, T. Kundu and J. Swenson (2016). Subsea separation-advanced subsea processing with linear pipe separators. Offshore Technology Conference, OnePetro.
- Shi, S.-y., J.-y. Xu, H.-q. Sun, J. Zhang, D.-h. Li and Y.-x. Wu (2012). "Experimental study of a vane-type pipe separator for oil-water separation." *Chemical Engineering Research and Design* **90**(10): 1652–1659.
- Skjefstad, H. and M. Stanko (2017). Subsea water separation: a state of the art review, future technologies and the development of a compact separator test facility. 18th International Conference on Multiphase Production Technology, OnePetro.
- Skjefstad, H. S. and M. Stanko (2018). An experimental study of a novel parallel pipe separator design for subsea oil-water bulk separation. SPE Asia Pacific Oil and Gas Conference and Exhibition, OnePetro.
- Skjefstad, H. S. and M. Stanko (2019). "Experimental performance evaluation and design optimization of a horizontal multi-pipe separator for subsea oil-water bulk separation." *Journal of Petroleum Science and Engineering* **176**: 203–219.
- Stanko, M. and M. Golan (2015). Simplified Hydraulic Design Methodology for a Subsea Inline Oil-Water Pipe Separator. *OTC Brasil*, OnePetro.